Communication

Selective Ion Passage through Functionalized Graphene Nanopores

Kyaw Sint, Boyang Wang, and Petr Kra#l

J. Am. Chem. Soc., **2008**, 130 (49), 16448-16449 • DOI: 10.1021/ja804409f • Publication Date (Web): 14 November 2008

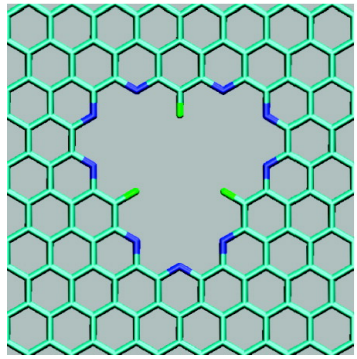

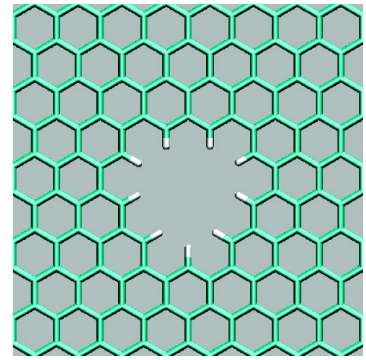

J|A|C|S
COMMUNICATIONS

Published on Web 11/14/2008

Selective Ion Passage through Functionalized Graphene Nanopores

Kyaw Sint, Boyang Wang, and Petr Král*

Department of Chemistry, University of Illinois at Chicago, Chicago, Illinois 60607

Received June 10, 2008; E-mail: pkral@uic.edu

Biological ionic channels play a key role in many cellular transport phenomena.[1] In their complex cores, these proteins contain precisely arranged arrays of charged amino acids that can efficiently recognize and guide the passing ions.[2] For industrial applications, much simpler nonbiological ionic and molecular channels can be made from zeolites,[3] carbon,[4] silica,[5] and other materials.[6,7] These channels are often not selective or transparent enough. Therefore, ion and molecular channels with novel structures[8] and recognition principles need to be designed.

Molecular dynamics studies have predicted[9] and experiments have demonstrated fast transport of gases[10,11] and liquids[12−15] through carbon nanotube (CNT) membranes. Hydrated ions could also pass through CNTs of large enough diameters.[16] Recently, graphene[17] and boron-nitride[18] monolayers have been prepared and intensively studied[19−21] for their many potential applications.

In this work, we design *functionalized nanopores* in graphene monolayers and show that they could serve as ionic sieves of high selectivity and transparency. In Figure 1, we display the studied chemically modified graphene nanopores. The F−N-pore (left) is terminated by negatively charged nitrogens and fluorines, favoring the passage of cations. The H-pore (right) is terminated by positively charged hydrogens, favoring the passage of anions. These nanopores might be formed in the graphene monolayers by ion etching,[22] and their chemical modifications could be realized by local oxidation, similarly as on graphene edges.[22,23]

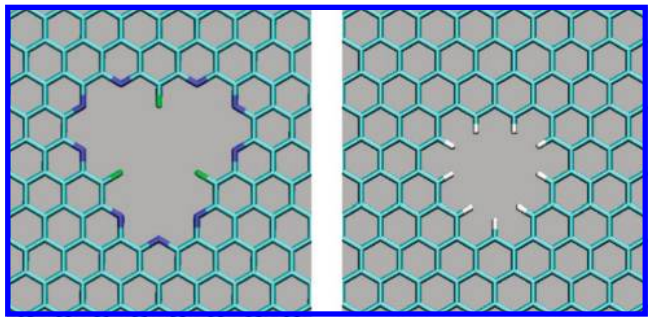

Figure 1. Functionalized graphene nanopores. (Left) The F−N-terminated nanopore. (Right) The H-terminated nanopore.

We model the passage of hydrated ions from the first and seventh periods through these nanopores by molecular dynamics (MD) simulations.[24] We use the NAMD package,[27] based on the CHARMM27 force field[28] (Supporting Information, SI). The model graphene sheets have chemically modified nanopores in their center with a diameter of ∼5 Å. The atomic charges of these sheets are obtained from first principle calculations with the B3LYP density functional using the Gaussian03 package,[29] as described in the SI. These calculations done without solvents show that when the ion passes through the graphene nanopore, the semimetallic sheet (screening length of 4 Å[30]) becomes highly polarized. Therefore, a screening charge of the same size but opposite sign to that of the ion goes to the pore rim and a neutralizing charge remains spread on the rest of the sheet. In the presence of water the screening charge should be more delocalized at the pore entrance, due to water polarization. In the MD simulations, we model these effects by homogeneously spreading the screening charge for the studied ion on the first atomic layer of the pore and the atomic ligands attached to it. The screening charge is kept there during the whole simulations, since its presence little affects the dynamics when the ion is far away from the pore. The opposite polarization charge on the sheet is neglected, for simplicity, so the combined system of the ion and the sheet is kept neutral.

In the MD simulations, the sheet is placed in a periodic unit cell with ∼10 Å of water on each side. One ion is placed in the cell and driven by an electric field E applied in the direction perpendicular to the graphene sheet. Each simulation run typically lasts 100−500 ns. It turns out that the F−N-pore is only passed by the Li^+, Na^+, and K^+ ions, while the H-pore is only passed by the Cl^- and Br^- ions. This selectivity of the nanopores, even in the presence of a large driving field of $E = 0.1$ V/nm, is caused by the Coulomb coupling between the ion and the functional groups attached to the nanopore rim. At this field, the passage rates of Li^+, Na^+, and K^+ have the ratio 9:14:33, while those of F^-, Cl^-, and Br^- have the ratio 0:17:33. Therefore, the nanopores are also highly selective to the sizes of the ions. The Li^+ and F^- ions have the lowest passage rates, because of their small radii and large coupling to the water molecules in their hydration shells. On the contrary, K^+ and Br^-

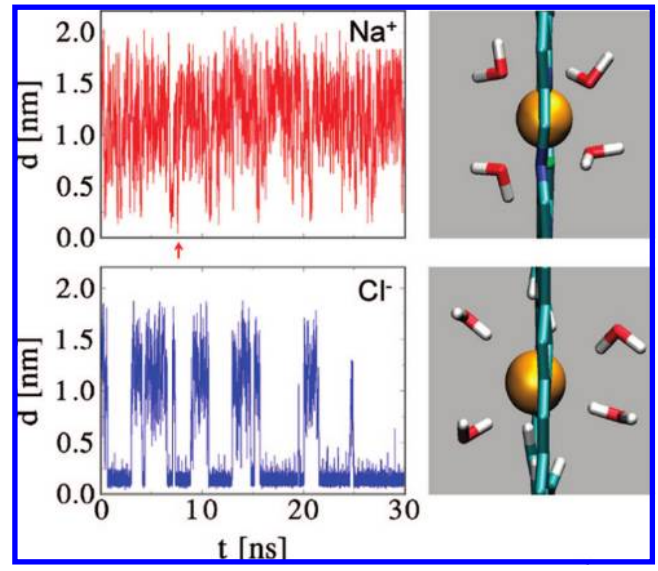

Figure 2. (Left) Time-dependent distance d between the Na^+ and Cl^- ions and the centers of the F−N-pore and H-pore, respectively, at the field of $E = 6.25$ mV/nm. Small arrow shows the only passage time of Na^+ through the F−N-pore. The dynamics of passage of these ions through the two pores is very different. (Right) While both ions are surrounded by two water "half-shells" when passing through their pores, only the Cl^- ion has relatively stable binding to the H-pore.

10.1021/ja804409f CCC: $40.75

have large radii, so it is relatively easy to break their hydration shells in the pores.

In Figure 2 (right insets), we show the configurations of the Na^+ and Cl^- ions passing through the two nanopores. The polar and charged nanopore rim can replace several water molecules from the first hydration shell of the ion passing through it. Therefore, the passing ion is surrounded by two separated first hydration "half-shells" at both sides. The close contact between the ion and the pore rim allows very efficient mapping and eventual removal of the ion shells. This leads to the high selectivity of the ion passage, as in channel proteins.

Figure 2 (left insets) displays the time-dependent distance d between the ions and their pore centers, obtained at a low field of $E = 6.25$ mV/nm. The distance fluctuations reveal a very different dynamics in both cases. The Na^+ ion passes the F−N-pore fast, without significantly binding with it. The ion rarely gets closer than 5 Å to the pore center and stays most of the time in the water region ($d > 10$ Å). The small vertical arrow shows the only passage observed of Na^+ in this time period. The ion passes through one of the three smaller holes in the nanopore with the C^3 symmetry. These asymmetric holes can not easily break the hydration shell of the Na^+ ion, which prohibits its prolonged stay in the pore. The K^+ ion binds weaker to its hydration shell, which can be more easily replaced by the pore rim, upon shell partial removal.

The Cl^- ion has even more stable binding to the symmetric H-pore, where it stays for ~70% of the time. At weak fields, the Cl^- ion enters and leaves the H-pore with almost the same rates from both sides. The electric field decreases the ion-pore binding, which is reflected in shorter time periods spent by the ion in the pore. At a field of $E = 0.1$ V/nm, the Cl^- ion stays in total only 30% of the time inside the pore.

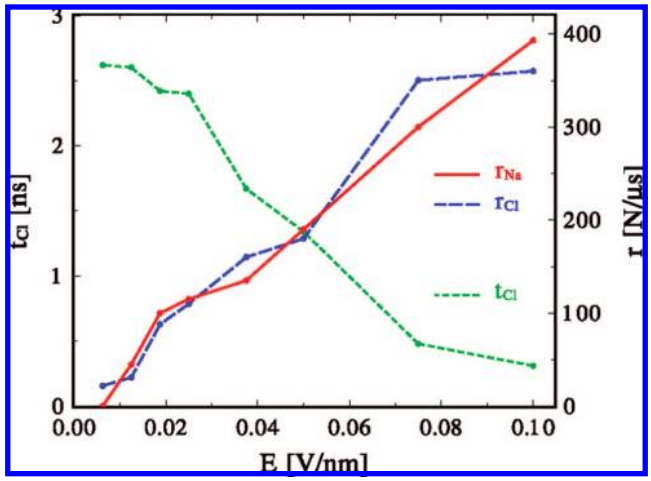

Figure 3. (Right axis) Dependence of the r_{Na} and r_{Cl} flow rates of the hydrated Na^+ and Cl^- ions through the F−N-pore and H-pore, respectively, on the applied electric field E. (Left axis) The average time t_{Cl} spent by the Cl^- ion inside the H-pore.

Figure 3 displays the field dependence of the average number of Na^+ and Cl^- ion passages, r_{Na} and r_{Cl}, through the F−N-pore and the H-pore, respectively. Both rates grow with the field, showing an accelerated passage of the ions through the pores and the surrounding water layers. We also present the average residence time t_{Cl} of the Cl^- ion in the H-pore, defined as the average time during which the ion stays within the 5 Å distance from the pore center once it enters the pore. One can see that t_{Cl} decreases with the electric field that breaks the Coulomb binding of the ion to the pore. The visible plateaus in the data reflect the structure of the potential barriers for the transfer of the ions through the pores.

The ion selectivity and passage rates through these nanopores could be optimized[31] by choosing the type of monolayer material, the size and shape of the nanopores, and the structure and number of functional ligands attached to their rim. Atomic monolayers with different types of nanopores might be arranged in dense arrays that would allow fast and efficient separation of different molecular species at the microscale and nanoscale. Such ultrasmall molecular sieves could revolutionize dialysis, desalination, and battery technologies.[32]

Acknowledgment. The work was done with the help of the NERSC and NCSA networks. K.S. and B.W. would like to acknowledge the support from the Paaren Fellowships.

Supporting Information Available: Two movies of the Na^+ and Cl^- ion passage through the F−N-pore and H-pore. This material is available free of charge via the Internet at http://pubs.acs.org.

References

(1) Ackerman, M. J.; Clapham, D. E. *N. Engl. J. Med* **1997**, *336*, 1575–1586.
(2) Yu, J.; Yool, A. J.; Schulten, K.; Tajkhorshid, E. *Structure* **2006**, *14*, 1411–1423.
(3) Jordan, E.; Bell, R. G.; Wilmer, D.; Koller, H. *J. Am. Chem. Soc.* **2006**, *128*, 558–567.
(4) Saufi, S. M.; Ismail, A. F. *Carbon* **2004**, *42*, 241–259.
(5) Duke, M. C.; da Costa, J. C. D.; Do, D. D.; Gray, P. G.; Lu, G. Q. *Adv. Funct. Mater.* **2006**, *16*, 1215–1220.
(6) Ghadiri, M. R.; Granja, J. R.; Buehler, L. K. *Nature* **1994**, *369*, 301–304.
(7) Kobuke, Y.; Ueda, K.; Sokabe, M. *J. Am. Chem. Soc.* **1992**, *114*, 7618–7622.
(8) Striemer, C. C.; Gaborski, T. R.; McGrath, J. L.; Fauchet, P. M. *Nature* **2007**, *445*, 749–753.
(9) Hummer, G.; Rasaiah, J. C.; Noworyta, J. P. *Nature* **2001**, *414*, 188–190.
(10) Skoulidas, A. I.; Ackerman, D. M.; Johnson, J. K.; Sholl, D. S. *Phys. Rev. Lett.* **2002**, *89*, 185901.
(11) Holt, J. K.; Park, H. G.; Wang, Y. M.; Stadermann, M.; Artyukhin, A. B.; Grigoropoulos, C. P.; Noy, A.; Bakajin, O. *Science* **2006**, *312*, 1034–1037.
(12) Majumder, M.; Chopra, N.; Andrews, R.; Hinds, B. J. *Nature* **2005**, *438*, 44.
(13) Wang, Z.; Ci, L.; Chen, L.; Nayak, S.; Ajayan, P. M.; Koratkar, N. *Nano Lett.* **2007**, *7*, 697–702.
(14) Zhou, J. J.; Noca, F.; Gharib, M. *Nanotechnology* **2006**, *17*, 4845–4853.
(15) Whitby, M.; Quirke, N. *Nat. Nanotechol.* **2007**, *2*, 87–94.
(16) Liu, H. M.; Murad, S.; Jameson, C. J. *J. Chem. Phys.* **2006**, *125*, 084713.
(17) Novoselov, K. S.; Geim, A. K.; Morozov, S. V.; Jiang, D.; Zhang, Y.; Dubonos, S. V.; Grigorieva, I. V.; Firsov, A. A. *Science* **2004**, *306*, 666–669.
(18) Corso, M.; Auwarter, W.; Muntwiler, M.; Tamai, A.; Greber, T.; Osterwalder, J. *Science* **2004**, *303*, 217–220.
(19) Geim, A. K.; Novoselov, K. S. *Nat. Mater.* **2007**, *6*, 183–191.
(20) Berner, S.; Corso, M.; Widmer, R.; Groening, O.; Laskowski, R.; Blaha, P.; Schwarz, K.; Goriachko, A.; Over, H.; Gsell, S.; Schreck, M.; Sachdev, H.; Greber, T.; Osterwalder, J. *Angew. Chem., Int. Ed.* **2007**, *46*, 5115–5119.
(21) Laskowski, R.; Blaha, P.; Gallauner, T.; Schwarz, K. *Phys. Rev. Lett.* **2007**, *98*, 106802.
(22) Stampfer, C.; Guttinger, J.; Molitor, F.; Graf, D.; Ihn, T.; Ensslin, K. *Appl. Phys. Lett.* **2008**, *92*, 012102.
(23) Stankovich, S.; Dikin, D. A.; Dommett, G. H. B.; Kohlhaas, K. M.; Zimney, E. J.; Stach, E. A.; Piner, R. D.; Nguyen, S. T.; Ruoff, R. S. *Nature* **2006**, *442*, 282–286.
(24) NVT ensemble with periodic boundary conditions is used, where the electrostatic coupling is calculated by the PME method.[25] The Langevin damping used, 0.01 ps^{-1}, minimizes the unphysical loss of momenta.[26]
(25) Darden, T.; York, D.; Pedersen, L. *J. Chem. Phys.* **1993**, *98*, 10089–10092.
(26) Wang, B.; Král, P. *J. Am. Chem. Soc.* **2006**, *128*, 15984–15985.
(27) Phillips, J. C.; Braun, R.; Wang, W.; Gumbart, J.; Tajkhorshid, E.; Villa, E.; Chipot, C.; Skeel, R. D.; Kale, L.; Schulten, K. *J. Comput. Chem.* **2005**, *26*, 1781–1802.
(28) Karplus, M.; et al. *J. Phys. Chem. B* **1998**, *102*, 3586–3617.
(29) Frisch, M. J.; et al. *Gaussian 03*, revision C.02; Gaussian, Inc.: Wallingford, CT, 2004.
(30) Ohta, T.; Bostwick, A.; Seyller, T.; Horn, K.; Rotenberg, E. *Science* **2006**, *313*, 951–954.
(31) Wang, B.; Král, P. *Small* **2007**, *3*, 580–584.
(32) Kim, S.; Marion, M.; Jeong, B. H.; Hoek, E. M. V. *J. Membr. Sci.* **2006**, *284*, 361–372.

JA804409F